Electrical transport properties of single-crystal antimony nanowire arrays

Y. Zhang, L. Li, G. H. Li,* and L. D. Zhang
Key Laboratory of Materials Physics, Anhui Key Laboratory of Nanomaterials and Nanotechnology, Institute of Solid State Physics, Chinese Academy of Sciences, Hefei 230031, People's Republic of China
(Received 7 November 2005; revised manuscript received 13 January 2006; published 22 March 2006)

Single crystalline Sb nanowire arrays with diameters ranging from 9 to 40 nm embedded in anodic alumina membranes were prepared by pulsed electrodeposition. Electrical transport measurements confirm the existence of the transition from a positive temperature coefficient of resistance to a negative one with decreasing diameter of the Sb nanowires. The weak localization effect is considered to play an important role in determining the temperature-dependent behavior of the resistance. The weak temperature dependence of the single crystalline Sb nanowire arrays might find application in constant resistance nanodevices.

DOI: 10.1103/PhysRevB.73.113403 PACS number(s): 73.63.−b, 82.45.Aa, 71.55.Ak

Nanowire systems have attracted a great deal of research interest because of their potential applications ranging from molecular electronics, thermoelectric devices to chemical sensors and their promise for studying the transport properties of one-dimensional (1D) systems. The quantum confinement of carriers in two dimensions normal to the wire axis significantly affects their electronic energy states, and makes the transport properties of these 1D systems very different from their bulk counterparts.[1–12] As a semimetal, Sb has an overlapped narrow band between the L points of the conduction bands and the T points of the valence bands. Compared with bismuth nanowires,[13–19] the semimetal-to-semiconductor transition is generally difficult to observe in Sb nanowires due to their higher carrier effective mass and larger energy overlap.[20] Nevertheless, the classical finite-size effect and quantum confinement effect are expected to be observed in Sb nanowires due to the large de Broglie wavelength (40 nm) and mean free path (a few microns).[21]

The transport properties of Sb nanowires strongly depend on the diameter and the crystal orientation of nanowires. Therefore, it is important to grow single crystalline Sb nanowire arrays with different diameters but with the same orientation, which will favor both electronic transport analysis and future device applications.

Here we report the electronic transport properties of [110] orientation Sb single crystalline nanowire arrays with diameters ranging from 9 to 40 nm fabricated by pulsed electrodeposition. The transition from a positive temperature coefficient of resistance to a negative one has been observed with decreasing nanowire diameter for the first time.

The fabrication of anodic alumina membranes (AAM) and the plating solution used for Sb nanowires growth is the same as that reported earlier.[22] The deposition was controlled by the unipolar pulse voltage in a common two-electrode electrochemical cell. The total cycle time of the pulse in each cycle is 1200 μs with the pulsed time of 400 μs and the delayed time of 800 μs. The optima growth conditions for single crystalline Sb nanowires with different diameters are listed in Table I.

Figure 1 shows the XRD patterns (D/MAX-rA with Cu K_α radiation) of the Sb nanowire arrays with different diameters. It can be seen that there is a very sharp diffraction peak at $2\theta=41.9°$, and other diffraction peaks are very weak, which demonstrates that all Sb nanowires have the same growth orientation. The single sharp peak corresponds to the $(11\bar{2}0)$ plane [or (110) plane] of the hexagonal Sb, indicating that the Sb nanowires with different diameters grow preferentially along the [110] crystal direction. Figure 2 shows a HRTEM image (JEOL 2010) of the 40 nm diameter Sb nanowire. Extremely high structural quality of the Sb nanowire can be seen from the clear image of two-dimensional lattice planes.

Figure 3 shows the temperature dependence of the resistance of single crystalline Sb nanowire arrays with different diameters [$R(T)$], normalized to the resistance at 273 K (a quasi-four-probe technique by attaching a voltage lead and a current lead to each side of the AAM). One can see that the resistances of the 40 nm and 30 nm Sb nanowires increase with temperature, which exhibits a positive temperature coefficient of resistance (TCR) and weak temperature dependence, i.e., a typical metal-like character. The $R(T)$ behaviors for the 15 nm (see also the inset in Fig. 3) and the 9 nm Sb nanowires exhibit a negative TCR, and the negative TCR is not exponential and has a semiconductorlike character. It is known that the TCR contributed by the localization can be positive or negative and depends on the diameter of the nanowires.[23] Factors contributing to the negative TCR may be complicated. We found that the resistance of the 9 nm Sb nanowires essentially follows a $T^{-1/2}$ law at temperatures lower than 110 K (see the dashed line in Fig. 3). It is known that both the carrier mobility and concentration contribute to the TCR value, and the two factors have opposite tempera-

TABLE I. Growth conditions for single crystalline Sb nanowire arrays with different diameters (J, current density; d, nanowire diameter; n, nanowire density; t, growth time).

J (mA/cm^2)	d (nm)	n (cm^{-2})	t (h)
12	40	2.9×10^{10}	18
10	30	4.7×10^{10}	7
4.7	15	2.6×10^{11}	0.5
4.2	9	2.9×10^{11}	0.3

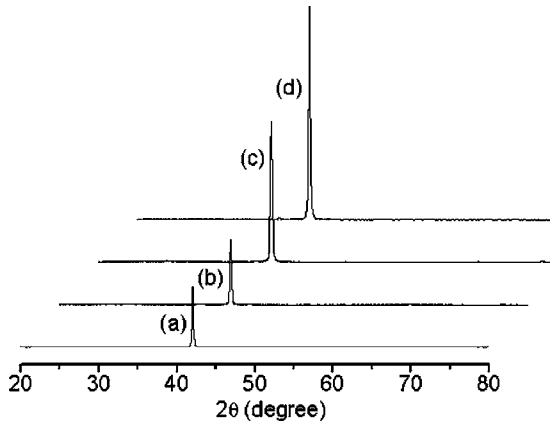

FIG. 1. XRD patterns of single crystalline Sb nanowire arrays with different diameters. (a) 40 nm, (b) 30 nm, (c) 15 nm, and (d) 9 nm.

ture dependence. For the 40 nm and 30 nm nanowires, the typical semimetal characteristics still remain and the carrier density is a weak function of temperature, thus the $R(T)$ is mainly controlled by the temperature dependence of the carrier mobility under the competition of various scattering mechanisms. The electron-boundary scattering, being relatively T independent, dominates at a lower temperature, and the electron-phonon scattering becomes dominant at a higher temperature and increases with temperature. Comparing to polycrystalline Sb nanowires with the similar diameters,[20] the single crystalline Sb nanowires exhibit weak temperature dependence in resistance. We deduce that, as in the case of Bi nanowires,[24] the phase-breaking length L_ϕ of single crystalline Sb nanowires is likely larger than that of polycrystalline Sb nanowires, thus the localization will be enhanced. The decrease in the diameter of the Sb nanowire will lead to a stronger finite size effect, which enhances the weak localization behavior at a lower temperature. The thermal excitation of carriers from the T-point valence band to the L-point conduction band will become important and can be observed at a lower temperature, especially for thinner Sb nanowires. This is why the weak localization of the resistance can be observed at a lower temperature for the single crystalline Sb nanowires with the diameters of 15 nm and 9 nm ($<$200 K for 15 nm and $<$110 K for 9 nm).

In addition, localization effects can also be typically evidenced in transverse magnetoresistance data of 30 nm single

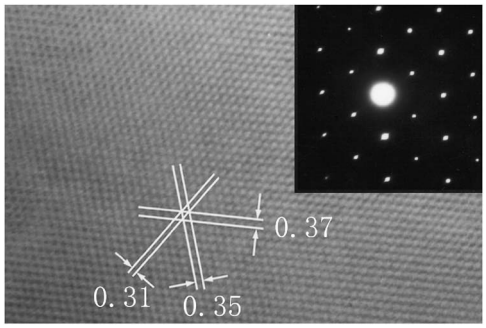

FIG. 2. HRTEM image of a single 40 nm Sb nanowire. The inset is the corresponding selective electron diffraction pattern.

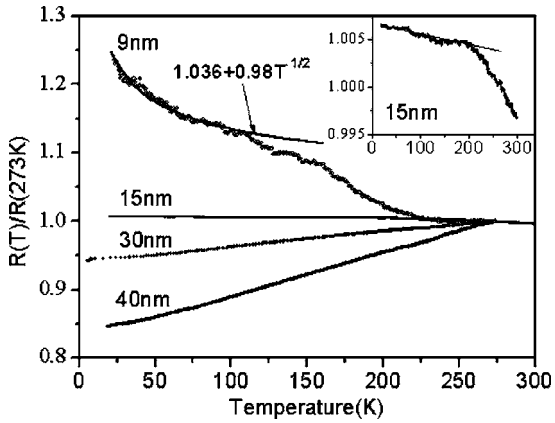

FIG. 3. Temperature dependence of the resistance of single crystalline Sb nanowire arrays with different diameters. The inset is a plot for 15 nm Sb nanowires.

crystalline Sb nanowires at 5 K (the magnetic field is perpendicular to the current direction), as shown in Fig. 4. For the 30 nm nanowires, a steplike increase in the magnetoresistance can be clearly observed at the low magnetic field, and then the magnetoresistance increases slowly with magnetic field. While for the 40 nm nanowires, almost a linear magnetic dependence of the magnetoresistance could be observed. It is known that the magnetic length, L_H, corresponding to the spatial extent of the wave function of the electrons in the lowest Landau level, can be described by[25]

$$L_H = \sqrt{\frac{3\hbar^2}{e^2AB^2}}, \tag{1}$$

where A is the cross-sectional area of the nanowire. At the critical magnetic field B_c, L_H is equal to d_w, the diameter of Sb nanowire, which gives B_c=0.45 T for the 30 nm Sb nanowire. Below B_c, the electron wave function is more confined by the nanowire walls than by the magnetic fields, and one-dimensional localization dominates. While above B_c, the Landau orbit size is smaller than the nanowire diameter, and the system becomes three-dimensional localization. Therefore, one can see that even the 30 nm single crystalline Sb nanowire behaves one-dimensionally at zero field. The decrease in the diameter of the Sb nanowires will enhance the

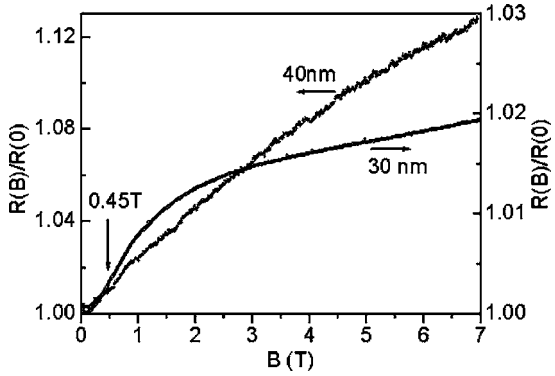

FIG. 4. Magnetic dependence of magnetoresistance for 30 nm and 40 nm single crystalline Sb nanowire arrays at 5 K.

one-dimensional localization behavior, and result in a negative temperature coefficient of resistance for 15 nm and 9 nm Sb nanowires.

In summary, single-crystalline Sb nanowire arrays highly oriented along the [110] direction with diameters of 9–40 nm have been prepared in anodic alumina membrane by the pulsed electrodeposition. An obvious transition from a positive temperature coefficient of resistance to a negative one has been observed in single-crystalline Sb nanowires arrays at the diameter of about 15 nm. The temperature-dependent behavior of resistance can be interpreted in terms of one-dimensional weak localization for 15 nm and 9 nm single crystalline Sb nanowire arrays. We observed the evidence of a transition from one-dimensional localization at low field to three-dimensional localization at high field for the 30 nm Sb nanowire at low temperatures from the measurement of the magnetoresistance. The weak localization plays an important role in determining the temperature dependence of the zero-field resistivity of the single crystalline Sb nanowires. The weak temperature dependence of the single crystalline Sb nanowire arrays might find application in constant resistance nanodevices.

This work was supported by the National Natural Science Foundation of China (No. 10474098) and the National Major Project of Fundamental Research for Nanomaterials and Nanostructures (No. 2005CB623603).

*Author to whom correspondence should be addressed. Electronic address: ghli@issp.ac.cn

[1] Y. M. Lin, O. Rabin, S. B. Cronin, J. Y. Ying, and M. S. Dresselhaus, Appl. Phys. Lett. **81**, 2403 (2002).
[2] Z. H. Zhong, D. L. Wang, Y. Cui, M. W. Bockrath, and C. M. Lieber, Science **302**, 1377 (2003).
[3] M. S. Martin-Gonázlez, G. J. Snyder, A. L. Prieto, R. Gronsky, T. Sands, and A. M. Stacy, Nano Lett. **3**, 973 (2003).
[4] Y. M. Lin and M. S. Dresselhaus, Appl. Phys. Lett. **83**, 3567 (2003).
[5] M. Chen, P. C. Searson, and C. L. Chien, J. Appl. Phys. **93**, 8253 (2003).
[6] L. Li, Y. Zhang, Y. W. Yang, X. H. Huang, G. H. Li, and L. D. Zhang, Appl. Phys. Lett. **87**, 031912 (2005).
[7] Y. Zhang, L. Li, and G. H. Li, Nanotechnology **16**, 2096 (2005).
[8] A. I. Hochbaum, R. Fan, R. R. He, and P. D. Yang, Nano Lett. **5**, 457 (2005).
[9] J. B. Cui and U. J. Gibson, Appl. Phys. Lett. **87**, 133108 (2005).
[10] L. Li, Y. W. Yang, X. H. Huang, G. H. Li, and L. D. Zhang, J. Phys. Chem. B **109**, 12394 (2005).
[11] T. E. Huber and M. J. Graf, Phys. Rev. B **60**, 16880 (1999).
[12] T. E. Huber and R. Calcao, 17th International Conference on Thermoelectrics (1998), p. 244.
[13] Z. B. Zhang, X. Z. Sun, M. S. Dresselhaus, J. Y. Ying, and J. P. Heremans, Appl. Phys. Lett. **73**, 1589 (1998).
[14] M. R. Black, M. Padi, S. B. Cronin, Y. M. Lin, O. Rabin, T. McClure, G. Dresselhaus, P. L. Hagelstein, and M. S. Dresselhaus, Appl. Phys. Lett. **77**, 4142 (2000).
[15] J. Heremans, C. M. Thrush, Y. M. Lin, S. Cronin, Z. Zhang, M. S. Dresselhaus, and J. F. Mansfield, Phys. Rev. B **61**, 2921 (2000).
[16] Y. M. Lin, S. B. Cronin, J. Y. Ying, M. S. Dresselhaus, and J. P. Heremans, Appl. Phys. Lett. **76**, 3944 (2000).
[17] X. F. Wang, J. Zhang, H. Z. Shi, Y. W. Wang, G. W. Meng, X. S. Peng, L. D. Zhang, and J. Fang, J. Appl. Phys. **89**, 3847 (2001).
[18] M. S. Sander, R. Gronsky, T. Sands, and A. M. Stacy, Chem. Mater. **15**, 335 (2003).
[19] L. Li, G. H. Li, Y. Zhang, Y. W. Yang, and L. D. Zhang, J. Phys. Chem. B **108**, 19380 (2004).
[20] J. Heremans, C. M. Thrush, Y. M. Lin, S. B. Cronin, and M. S. Dresselhaus, Phys. Rev. B **63**, 085406 (2001).
[21] J. H. Xu and C. S. Ting, Appl. Phys. Lett. **63**, 129 (1993).
[22] Y. Zhang, G. H. Li, Y. C. Wu, B. Zhang, W. H. Song, and L. D. Zhang, Adv. Mater. (Weinheim, Ger.) **14**, 1227 (2002).
[23] D. E. Beutler and N. Giordano, Phys. Rev. B **38**, 8 (1988).
[24] J. Heremans, C. M. Thrush, Z. Zhang, X. Sun, M. S. Dresselhaus, J. Y. Ying, and D. T. Morelli, Phys. Rev. B **58**, R10091 (1998).
[25] J. P. Heremans, C. M. Thrush, D. T. Morelli, and M.-C. Wu, Phys. Rev. Lett. **91**, 076804 (2003).